

# Measurement of the energy dependence of $\sigma_{\text{tot}}(\gamma p)$ with the ZEUS detector at HERA

Amir Stern for the ZEUS Collaboration

School of Physics and Astronomy, Tel Aviv University, 69978 Tel Aviv, Israel

DOI: <http://dx.doi.org/10.5689/UA-PROC-2010-09/37>

The energy dependence of the photon-proton total cross section,  $\sigma_{\text{tot}}(\gamma p)$ , was determined from  $e^+p$  scattering data collected with the ZEUS detector at HERA at three values of the center-of-mass energy,  $W$ , of the  $\gamma p$  system in the range  $194 < W < 296$  GeV. This is the first determination of the  $W$  dependence of  $\sigma_{\text{tot}}(\gamma p)$  from a single experiment at high  $W$ . Parameterizing  $\sigma_{\text{tot}}(\gamma p) \propto W^{2\epsilon}$ ,  $\epsilon = 0.111 \pm 0.009$  (stat.)  $\pm 0.036$  (syst.) was obtained.

## 1 Introduction

Donnachie and Landshoff (DL) [1] showed that the energy dependence of all hadron-hadron total cross sections can be described by a simple Regge motivated form,

$$\sigma_{\text{tot}} = A \cdot (W^2)^\epsilon + B \cdot (W^2)^{-\eta}, \quad (1)$$

where  $A$  and  $B$  are process-dependent constants,  $W$  is the hadron-hadron center-of-mass energy, and  $\epsilon (= \alpha_P(0) - 1)$  and  $\eta (= 1 - \alpha_R(0))$  are effective powers related to Pomeron and Reggeon exchange, respectively ( $\alpha_P(0)$  ( $\alpha_R(0)$ ) is the Pomeron (Reggeon) trajectory intercept).

The  $\sigma_{\text{tot}}(\gamma p)$  dependence on  $W$  is particularly interesting because of the nature of the photon, which is known to exhibit properties of both a point-like particle (direct photon) and a hadron-like state (resolved photon). At the  $ep$  collider HERA,  $\sigma_{\text{tot}}(\gamma p)$  can be extracted from  $ep$  scattering at very low squared momentum transferred at the electron vertex,  $Q^2 \lesssim 10^{-3}$  GeV<sup>2</sup>.

The measurements of the total  $\gamma p$  cross section at HERA for  $W \simeq 200$  GeV [2, 3, 4, 5, 6] combined with measurements at low  $W$  confirmed that the total photoproduction cross section has a  $W$  dependence similar to that of hadron-hadron reactions. However, the HERA measurements' systematic uncertainties were too large for a precise determination of the  $W$  dependence of the cross section. The original fits of DL gave  $\epsilon = 0.0808$  and no uncertainties were determined. Cudell et al. [7] determined  $\epsilon$  to be  $0.093 \pm 0.003$ . However, only very few points were present for the highest center-of-mass energies. The data were from different experiments and had a large spread. Furthermore, the value of the Pomeron intercept comes out strongly correlated with that of the reggeon trajectories. In another evaluation [8], the authors give the range of 0.07–0.10 as acceptable values for  $\epsilon$ .

In the final months of operation, the HERA collider was run with constant nominal positron energy, and switched to two additional proton energies, 460 GeV and 575 GeV, lower than the nominal value of 920 GeV. This opened up the possibility to determine precisely the power of the  $W$  dependence of  $\sigma_{\text{tot}}(\gamma p)$  from ZEUS data alone, in the range 194–296 GeV by measuring the ratios of cross sections, thus having many of the systematic uncertainties canceling out.

The difficulty in measuring total cross section,  $\sigma$ , in a collider environment originates from the limited acceptance of collider detectors for certain class of processes, in particular for elastic and diffractive scattering, where the final state particles are likely to disappear down the beam-pipe. The determination of the acceptance relies on Monte Carlo simulation of the physics and of the detector. The simulation of the physics is subject to many uncertainties which then impact on the systematic uncertainty of the cross section measurement. For the energy dependence of  $\sigma$ , the impact of these uncertainties as well as of the geometrical uncertainties can be minimized by studying the ratio  $r$  of cross sections probed at different  $W$  values. Assuming  $\sigma \sim W^{2\epsilon}$  [6],

$$r = \frac{\sigma(W_1)}{\sigma(W_2)} = \left( \frac{W_1}{W_2} \right)^{2\epsilon}. \quad (2)$$

Experimentally,

$$\sigma = \frac{N}{A \cdot \mathcal{L}}, \quad (3)$$

where  $A$ ,  $\mathcal{L}$  and  $N$  are the acceptance, luminosity and number of measured events, respectively, and therefore

$$r = \frac{N_1}{N_2} \cdot \frac{A_2}{A_1} \cdot \frac{\mathcal{L}_2}{\mathcal{L}_1}, \quad (4)$$

where the index 1(2) denotes measurements performed at  $W_1$  ( $W_2$ ). The acceptance for  $\gamma p$  events at HERA depends mainly on the detector infrastructure in the positron (rear) direction. If the change in the  $W$  value results from changing the proton energy, the acceptance is likely to remain the same, independently of  $W$ , and the ratio of acceptances will drop out of formula (4).

## 2 Kinematics and cross section

The photon-proton total cross section can be measured in the process  $e^+p \rightarrow e^+\gamma p \rightarrow e^+X$ , where the interacting photon is almost real. The event kinematics may be described in terms of Lorentz-invariant variables: the photon virtuality,  $Q^2$ , the event inelasticity,  $y$ , and the square of the photon-proton center-of-mass energy,  $W$ , defined by

$$Q^2 = -q^2 = -(k - k')^2, \quad y = \frac{p \cdot q}{p \cdot k}, \quad W^2 = (q + p)^2,$$

where  $k$ ,  $k'$  and  $p$  are the four-momenta of the incoming positron, scattered positron and incident proton, respectively, and  $q = k - k'$ . These variables can be expressed in terms of the experimentally measured quantities

$$Q^2 = Q_{\min}^2 + 4E_e E'_e \sin^2 \frac{\theta_e}{2}, \quad y = 1 - \frac{E'_e}{E_e} \cos^2 \frac{\theta_e}{2} \simeq 1 - \frac{E'_e}{E_e}, \quad W \simeq 2\sqrt{E_e E_p y},$$

where  $Q_{\min}^2 = \frac{m_e^2 y^2}{1-y}$ ,  $E_e$ ,  $E'_e$  and  $E_p$  are the energies of the incoming positron, scattered positron and incident proton, respectively,  $\theta_e$  is the positron scattering angle with respect to the initial positron direction and  $m_e$  is the positron mass. The scattered positron was detected in a positron tagger close to the beam line, restricting  $\theta_e$  (and hence  $Q^2$ ) to small values. The photon virtuality ranged from the kinematic minimum,  $Q_{\min}^2 \simeq 10^{-6}$  GeV<sup>2</sup>, up to  $Q_{\max}^2 \simeq 10^{-3}$  GeV<sup>2</sup>, determined by the acceptance of the positron tagger.

The  $\gamma p$  cross-section can be determined from the measured number of  $e^+p$  events using the following formula:

$$\frac{d\sigma^{e^+p}(y)}{dy} = \frac{\alpha}{2\pi} \left[ \frac{1 + (1-y)^2}{y} \ln \frac{Q_{\max}^2}{Q_{\min}^2} - 2 \frac{(1-y)}{y} \left(1 - \frac{Q_{\min}^2}{Q_{\max}^2}\right) \right] \sigma_{\text{tot}}^{\gamma p}(y), \quad (5)$$

where  $\alpha$  is the electromagnetic coupling constant. The term multiplying the  $\gamma p$  cross-section is known as the flux factor.

For each of the incident proton energies,  $\sigma_{\text{tot}}^{\gamma p}(y)$  has a small variation as a function of  $y$  over the range of the measurement and may be taken to be a constant,  $\sigma_{\text{tot}}^{\gamma p}$ . Thus, the flux may be integrated over the range of measurement to give a total flux  $F_\gamma$ , which, when multiplied by the total  $\gamma p$  cross section gives  $\sigma_{\text{tot}}^{ep}$ , the ep cross section integrated over the measured range,

$$\sigma_{\text{tot}}^{ep} = F_\gamma \cdot \sigma_{\text{tot}}^{\gamma p}. \quad (6)$$

### 3 Experimental setup

In the final days of HERA running, 27.5 GeV positrons were colliding with protons of energy set at the nominal value of 920 GeV (high energy run, HER) and lowered to 575 (medium energy run, MER) and 460 GeV (low energy run, LER).

The ZEUS detector components used in this analysis are the main calorimeter (CAL) that consisted of three parts: the forward (FCAL), the barrel (BCAL) and the rear (RCAL) calorimeters, the central tracking detector (CTD), the microvertex detector (MVD), the six meter tagger (TAG6) and the luminosity monitoring system. The TAG6 was a spaghetti type calorimeter located 5.7 m from the interaction point in the backward direction and was used for tagging photoproduction events. Scattered positrons were bent into it by the first HERA dipole and quadrupole magnets after the interaction region, with full acceptance for positrons with zero transverse momentum in the approximate energy range 3.8–7.1 GeV with a  $y$  range of 0.74–0.86. The luminosity collected in the ZEUS detector was determined by two independent systems, the photon calorimeter (PCAL) and the spectrometer (SPEC), that measured the rate of the Bethe-Heitler (BH) process ( $e^+p \rightarrow e^+\gamma p$ ). The PCAL was shielded from primary synchrotron radiation by two carbon filters, each approximately two radiation lengths deep. Each filter was followed by an aerogel Cherenkov detector (AERO) to measure the energy of showers starting in the filters. The two components (PCAL and SPEC) enabled the measurement of the luminosity in two independent ways with 1% relative uncertainty. A schematic layout of the detector is shown in Fig. 1.

A special photoproduction trigger was implemented, requiring a low-angle scattered positron candidate detected in the TAG6 and some activity in RCAL. To reduce the background from events with energy in RCAL and a TAG6 hit caused by a random coincidence with a BH event in the same HERA bunch, the energy in the PCAL,  $E_{\text{PCAL}}$ , was restricted to  $E_{\text{PCAL}} \lesssim 14$  GeV.

The PYTHIA 6.416 [9] generator, coupled to the HERACLES 4.6 [10, 11] program (to simulate electromagnetic radiative effects), was used to simulate the photoproduction processes in the proper weight to describe the CAL energy distributions in the total-cross-section data.

The acceptance for  $\gamma p$  events is determined by the acceptance of the TAG6 and that of the main detector, which are independent. The above mentioned simulation was used to calculate the acceptance of the RCAL for photoproduction processes.

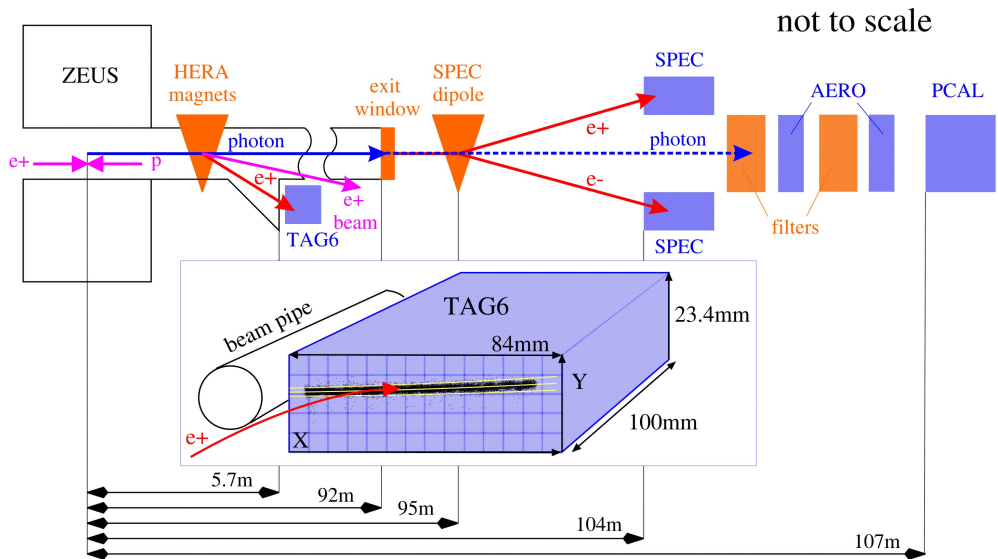


Figure 1: Schematic layout of the ZEUS detector, the six meter tagger and the components of the luminosity system and their distance from the interaction point.

## 4 Event selection and data analysis

Clean positron hits in the TAG6 were selected by requiring that the highest-energy cell was not at the edge of the detector. Showers from inactive material in front of the tagger were rejected by a cut on the energy sharing among towers surrounding the tower with highest energy. The position of the positron was reconstructed by a neural network trained on an MC simulation of the TAG6 [12]. The neural-network method was also used to correct the energy of the positrons for a small number of noisy cells, which were excluded. Events from the BH process, selected by requiring a positron in the TAG6 in coincidence with a photon in the SPEC, were used to calibrate the TAG6 with positrons with very small transverse momentum. The energy,  $E$ , was determined as a function of the horizontal position,  $X$ , and the correlation between  $X$  and the vertical position,  $Y$ , was also measured. Cuts were placed on  $E(X)$  and  $Y(X)$  for the photoproduction events to reject positrons with transverse momentum  $p_T \gtrsim 10$  MeV, off-momentum beam positrons, and background from beam-gas interactions [12]. The  $(X, Y)$  distribution of positrons from a sample of BH events from the MER, and the  $Y(X)$  cuts, are shown in the inset in Fig. 1.

In RCAL, the towers immediately horizontally adjacent to the beam-pipe hole had a large rate from off-momentum beam positrons and debris from beam-gas interactions which satisfied the trigger conditions. In events in which the RCAL cell with highest energy was in one of these towers, the fraction of total RCAL energy,  $E_{\text{RCAL}}$ , in that tower was required to be below an  $E_{\text{RCAL}}$ -dependent threshold [12]. This eliminated most of the background and resulted in only about 2.9% loss of signal events.

Background from positron beam-gas interactions passing the trigger requirement was determined from non-colliding HERA positron bunches. This sample was subtracted statistically from the colliding HERA bunches by the ratio of currents of  $ep$  bunches to  $e$ -only bunches.

Photoproduction events associated with the TAG6 hit could have a random coincidence with an event in the same HERA bunch from the BH process, with the BH photon depositing more than 14 GeV in the PCAL and therefore vetoing the event. To account for this loss, accepted events were weighted by a factor determined from the rate of overlaps at the time the event was accepted. The fraction of overlaps is proportional to the instantaneous luminosity, which was higher during the HER relative to the LER and MER. The correction for this effect was  $\approx +2.6\%$  for the HER and  $\approx +1.2\%$  for the LER and MER data samples.

Another background came from photoproduction events outside the  $W$  range of the TAG6 but satisfying the RCAL trigger, with a random coincidence from BH hitting the TAG6. The photon from the BH event may not have been vetoed by the  $E_{\text{PCAL}} \lesssim 14$  GeV requirement due to the limited acceptance and resolution of the PCAL. Such overlaps were studied using the distribution of the energy of the PCAL+AERO; this offered greatly improved photon energy resolution over the PCAL alone. In addition to the BH events which produced a TAG6 hit, this spectrum also contained photoproduction events associated with the TAG6 hit overlapping in the same HERA bunch with a photon from a random BH event whose positron did not hit the TAG6. The number of overlaps seen in the PCAL, corrected for the PCAL acceptance, was the number of BH overlaps to subtract from the selected photoproduction sample.

## 5 Results

The total photon-proton cross section for one proton energy is given by

$$\sigma_{\text{tot}}^{\gamma p} = \frac{N}{A_{\text{RCAL}} \cdot F_{\gamma}^{\text{TAG6}} \cdot \mathcal{L}}, \quad (7)$$

where  $N$  is the measured number of events,  $\mathcal{L}$  is the integrated luminosity,  $F_{\gamma}^{\text{TAG6}}$  is the fraction of the photon flux tagged by the TAG6, and  $A_{\text{RCAL}}$  is the acceptance of the hadronic final state for tagged events.

The acceptance of the detector for all three energy settings was found to be equal within errors and thus their ratio cancels. The data taken correspond to a luminosity of 567 nb<sup>-1</sup> in the HER, 949 nb<sup>-1</sup> in the MER and 912 nb<sup>-1</sup> in the LER.

In Fig. 2 the measured relative values of  $\sigma_{\text{tot}}^{\gamma p}$  are shown as a function of  $W$ , where the cross section for HER is normalized to unity. A fit of the form  $W^{2\epsilon}$  was performed to the relative cross sections using only the statistical uncertainties, and separately with all the uncorrelated systematic uncertainties added in quadrature. The correlated shifts were then applied to the data and the fit repeated; the change in  $\epsilon$  was negligible. The result for the logarithmic derivative in  $W^2$  of the energy dependence is

$$\epsilon = 0.111 \pm 0.009 \text{ (stat.)} \pm 0.036 \text{ (syst.)}.$$

This result is consistent with earlier determinations of  $\epsilon$ , however has the advantage of being obtained from a single experiment.

In the picture in which the photoproduction cross section is  $\propto \ln^2(W^2)$  as required by the Froissart bound [13],  $\epsilon \approx 0.11$  is expected, in agreement with the present measurement. The interpretation of this result in terms of the Pomeron intercept is subject to assumptions on the Reggeon contribution in the relevant  $W$  range. The most recent analysis of all hadronic cross sections using a fit taking into account Pomeron and Reggeon terms [14] yielded a Pomeron intercept of  $0.0959 \pm 0.0021$ . This is in agreement with the result presented here.

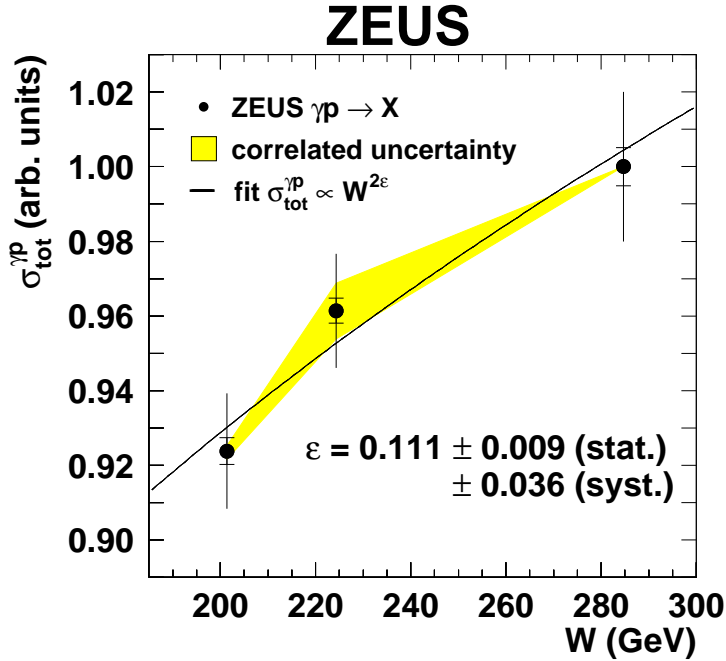


Figure 2: The  $W$  dependence of the total photon-proton cross section, normalized to the value for the HER. The inner error bars show the statistical uncertainties of the total-cross-section data; the outer error bars show those uncertainties and all uncorrelated systematic uncertainties added in quadrature. The shaded band shows the effect of the correlated systematic uncertainties. The curve shows the fit to the form  $\sigma_{\text{tot}}(\gamma p) \propto W^{2\epsilon}$ .

## References

- [1] A. Donnachie and P. V. Landshoff, Phys. Lett. B **296** (1992) 227 [arXiv:hep-ph/9209205].
- [2] M. Derrick *et al.* [ZEUS Collaboration], Phys. Lett. B **293** (1992) 465.
- [3] T. Ahmed *et al.* [H1 Collaboration], Phys. Lett. B **299** (1993) 374.
- [4] M. Derrick *et al.* [ZEUS Collaboration], Z. Phys. C **63** (1994) 391.
- [5] S. Aid *et al.* [H1 Collaboration], Z. Phys. C **69** (1995) 27 [arXiv:hep-ex/9509001].
- [6] S. Chekanov *et al.* [ZEUS Collaboration], Nucl. Phys. B **627** (2002) 3 [arXiv:hep-ex/0202034].
- [7] J. R. Cudell, V. Ezhela, K. Kang, S. Lugovsky and N. Tkachenko, Phys. Rev. D **61** (2000) 034019 [Erratum-ibid. D **63** (2001) 059901] [arXiv:hep-ph/9908218].
- [8] J. R. Cudell, K. Kang and S. K. Kim, Phys. Lett. B **395** (1997) 311 [arXiv:hep-ph/9601336].
- [9] T. Sjostrand, Z. Phys. C **42** (1989) 301.  
H. U. Bengtsson and T. Sjostrand, Comput. Phys. Commun. **46** (1987) 43.
- [10] A. Kwiatkowski, H. Spiesberger and H.-J. Möhring, Computer Phys. Comm. **69** (1992) 155.
- [11] H. Spiesberger, "HERACLES, An event generator for  $ep$  interactions at HERA including radiative processes (Version 4.6)" (1996), available on <http://www.desy.de/~hspiesb/heracles.html>.
- [12] O. Gueta, M.Sc. Thesis, Tel Aviv University, Report DESY-THESIS-2010-030, 2010.
- [13] M. Froissart, Phys. Rev. **123** (1961) 1053.  
A. Martin, Nuovo Cim. A **42** (1965) 930.
- [14] J. R. Cudell *et al.*, Phys. Rev. D **65** (2002) 074024 [arXiv:hep-ph/0107219].